Extremophiles (2011) 15:245–252
DOI 10.1007/s00792-010-0352-1

ORIGINAL PAPER

Mutational analysis of conserved aspartic acid residues in the *Methanothermobacter thermautotrophicus* MCM helicase

Nozomi Sakakibara · Rajesh Kasiviswanathan · Zvi Kelman

Received: 25 June 2010 / Accepted: 22 December 2010 / Published online: 28 January 2011

Abstract Minichromosome maintenance (MCM) helicases are thought to function as the replicative helicases in archaea and eukarya, unwinding the duplex DNA in the front of the replication fork. The archaeal MCM helicase can be divided into three parts, the N-terminal, catalytic, and C-terminal regions. The N-terminal part of the protein is divided into three domains, A, B, and C, and was shown to be involved in protein multimerization and binding to single- and double-stranded DNA. Two Asp residues found in domain C are conserved among MCM proteins from different archaea. These residues are located in a loop at the interface with domain A. Mutations of these residues in the *Methanothermobacter thermautotrophicus* MCM protein, Asp202 and Asp203, to Asn result in a significant reduction in the ability of the enzyme to bind DNA and in lower thermal stability. However, the mutant proteins retained helicase and ATPase activities. Further investigation of the DNA binding revealed that the presence of ATP rescues the DNA binding deficiencies by these mutant proteins. Possible roles of these conserved residues in MCM function are discussed.

Keywords Archaea · DNA replication · MCM helicase · *Methanothermobacter thermautotrophicus*

Abbreviations

CD	Circular dichroism
dsDNA	Double-stranded DNA
DSC	Differential scanning calorimetry
MCM	Minichromosome maintenance
mt	*Methanothermobacter thermautotrophicus*
ssDNA	Single-stranded DNA

Introduction

Minichromosome maintenance (MCM) helicase is thought to function as the replicative helicase, and to unwind the duplex DNA ahead of the replication fork. Most archaea sequenced contain a single MCM homolog, while some archaea contain up to eight homologs (Kelman and Kelman 2003; McGeoch and Bell 2008; Sakakibara et al. 2009a). The MCM protein from the archaeon *Methanothermobacter thermautotrophicus* (mt) has been extensively studied. mtMCM possesses helicase activity with $3' \rightarrow 5'$

Communicated by L. Huang.

N. Sakakibara · R. Kasiviswanathan
Center for Advanced Research in Biotechnology, University of Maryland Biotechnology Institute, 9600 Gudelsky Drive, Rockville, MD 20850, USA

Z. Kelman
Institute for Bioscience and Biotechnology Research, 9600 Gudelsky Drive, Rockville, MD 20850, USA

Z. Kelman
Department of Cell Biology and Molecular Genetics, University of Maryland, College Park, MD 20742, USA

Present Address:
N. Sakakibara (✉)
Laboratory of Viral Diseases, NIAID, NIH, 4 Center Drive, Bethesda, MD 20892, USA
e-mail: sakakibaran@niaid.nih.gov

Present Address:
R. Kasiviswanathan
Laboratory of Molecular Genetics, National Institute of Environmental Health Sciences, 111 TW Alexander Dr., Research Triangle Park, NC 27709, USA

directionality, has a DNA-dependent ATPase activity, can translocate along single-stranded (ss) and double-stranded (ds) DNA, can unwind a DNA–RNA hybrid duplex substrate when translocating on the DNA strand, and can displace proteins from DNA (reviewed in Sakakibara et al. 2009a). mtMCM is a 76 kDa protein and can form several oligomeric structures including dodecamers, heptamers, hexamers and filaments (Costa and Onesti 2009; Sakakibara et al. 2009a; Brewster and Chen 2010). The archaeal MCM proteins can be divided into three major parts: a N-terminal region, a center part which includes the catalytic domains, and a C-terminal region proposed to form a helix-turn-helix motif (Brewster et al. 2008; Bae et al. 2009). The three-dimensional structure of the N-terminal part revealed a three domain structure: A, B, and C (Fig. 1a; Fletcher et al. 2003; Liu et al. 2008). Domain A is mostly α-helical and has been suggested to participate in regulating helicase activity. Domain B consists of three β-sheets and contains a zinc finger motif which plays a role in DNA binding (Poplawski et al. 2001; Kasiviswanathan et al. 2004). Domain C consists of a canonical oligonucleotide/oligosaccharide binding (OB) fold with an extended β-hairpin that protrudes toward the central cavity. The β-hairpin is required for DNA binding (Fletcher et al. 2003; Kasiviswanathan et al. 2006). Domain C was also shown to participate in mtMCM oligomerization and to communicate between the N-terminal DNA binding part and the catalytic region (Kasiviswanathan et al. 2004; Sakakibara et al. 2008).

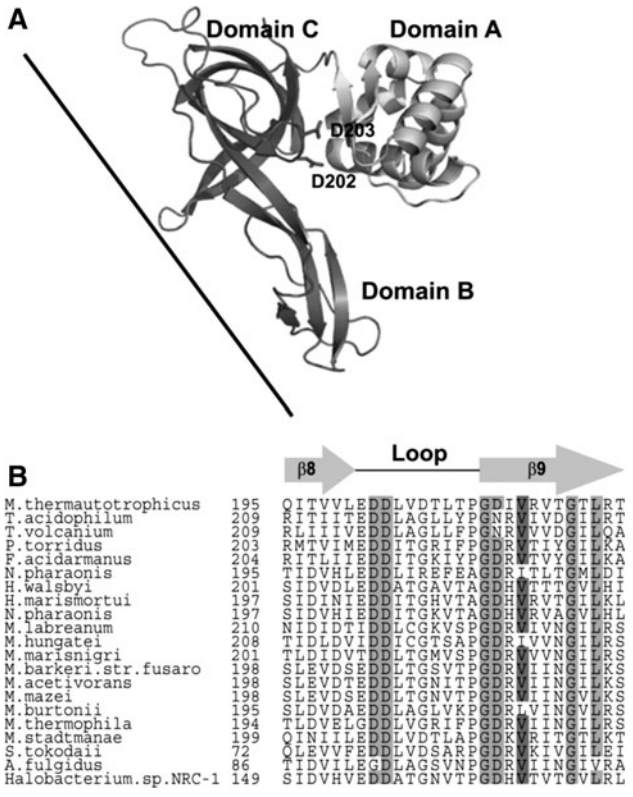

Fig. 1 Location and conservation of mtMCM Asp202 and Asp203. **a** The structure of the N-terminal part of the mtMCM helicase. The three domains and the D202 and D203 residues are marked. The location of the DNA in the central cavity is represented by a *line*. PyMOL was used to construct the figure (PDBID: 1LTL). **b** An alignment of the loop between β8 and β9 from several archaeal MCM proteins. Residues identical in more than 90% of the proteins are highlighted in *light gray* and those in more than 80% are highlighted in *dark gray*

Alignment of archaeal MCM protein sequences revealed that there are two highly conserved Asp residues at positions 202 and 203 (in mtMCM) which are part of domain C (Fig. 1a). These residues are located in the loop between β8 and β9 and positioned at the interface between domains A and C (Fig. 1a, b). In general, unless required for a specific function, loop regions in proteins are less conserved than more structured regions. Thus, the role of the two conserved Asp residues was investigated. Both Asp residues were mutated to Asn and the biochemical properties of the mutant proteins were determined. The mutations result in decreased DNA binding and thermostability of the proteins. However, in the presence of ATP DNA binding activity was restored.

Materials and methods

Materials

ATP and [γ-^{32}P]ATP were obtained from GE Healthcare, and oligonucleotides were synthesized by the NIST/UMD DNA synthesis facility.

Construction, expression and purification of MCM mutant proteins

mtMCM mutant proteins were generated using PCR-based site-directed mutagenesis as previously described (Kasiviswanathan et al. 2004). All constructs contain a C-terminal His_6-tag and were cloned into the *Nde*I and *Xho*I sites of the pET-21a vector (Novagen). The oligonucleotides containing the point mutations (underlined nucleotide) for introducing the D202N mutation in MCM are 5′-CAG ATA ACA GTT GTC CTG GAG AAC GAC CTG GTT GAC ACC CTC ACA CCC-3′ and 5′-GGG TGT GAG GGT GTC AAC CAG GTC GTT CTC CAG GAC AAC TGT TAT CTG-3′; for the D203N mutation they are 5′-CAG ATA ACA GTT GTC CTG GAG GAC AAC CTG GTT GAC ACC CTC ACA CCC-3′ and 5′-GGG TGT GAG GGT GTC AAC CAG GTT GTC CTC CAG GAC AAC TGT TAT CTG-3′; for DD202,203NN they are 5′-GTT GTC CTG GAG AAC AAC CTG GTT GAC ACC CTC-3′ and 5′-GAG GGT GTC AAC CAG GTT GTT CTC CAG GAC AAC-3′. All constructs were

confirmed by DNA sequencing. The wild-type and mutant proteins were overexpressed in BL21(DE3) CodonPlus cells (Stratagene) at 37°C and purified on a Ni-column as previously described (Shin et al. 2003a).

ATPase assay

ATPase activity was measured in reaction mixtures (15 μl) containing 25 mM Hepes–NaOH (pH 7.5), 1 mM dithiothreitol, 5 mM $MgCl_2$, 100 μg/ml BSA, and 1,500 pmol of [γ-^{32}P]ATP (3,000 Ci/mmol; GE Healthcare) and 30 or 90 nM MCM protein (as monomer) in the presence or absence of 50 ng ssDNA (5′-GGCAGATAACAGTTGTCCTGGAGAACGACCTGGTTGACACCCTCACACCC-3′). After incubation at 60°C for 60 min, samples were placed on ice, then an aliquot (1 μl) was spotted onto a polyethyleneimine cellulose thin layer plate, and ATP and P_i were separated by chromatography in 1 M formic acid and 0.5 M LiCl. The extent of ATP hydrolysis was quantitated by phosphorimager analysis. All ATPase assays were repeated three times, and their averages with standard deviations are shown in Fig. 4b.

Gel filtration

One hundred micrograms of wild-type or mutant MCM proteins was applied to a superose-6 gel filtration column (HR10/30, GE Healthcare) pre-equilibrated with buffer containing 20 mM Tris–HCl (pH 7.5), 150 mM NaCl, and 10% glycerol. The column was run at a flow rate of 0.2 ml/min at 22°C. The presence of protein was determined by ultraviolet absorbance at 280 nm.

Nitrocellulose filter DNA binding assay

Single-stranded and dsDNA substrates for filter binding assays were prepared by labeling the oligonucleotide using [γ-^{32}P]ATP and T4 polynucleotide kinase. Unincorporated [γ-^{32}P]ATP was removed by extracting the DNA substrate from a polyacrylamide gel as previously described (Shin and Kelman 2006). For ssDNA binding, a 49mer oligonucleotide with the sequence 5′-GCAGATAACAGTTGTCCTGGAGAACGACCTGGTTGACACCCTCACACCC-3′ was used. For dsDNA, the same oligonucleotide was hybridized to its complementary sequence. For forked DNA substrates, two 49mer oligonucleotides with the sequences 5′-TTTGTTTGTTTGTTTGTTTGTTTGCCGACGTGCCAGGCCGACGCGTCCC-3′ and 5′-GGGACGCGTCGGCCTGGCACGTCGGTTTGTTTGTTTGTTTGTTTTGTTTG-3′ were hybridized to form the substrate.

Filter binding assays were carried out in a reaction mixture (20 μl) containing 25 mM Hepes–NaOH (pH 7.5), 2 mM dithiothreitol, 10 mM $MgCl_2$, 100 μg/ml BSA, 50 fmol of ^{32}P-labeled ss or dsDNA substrates, and 10, 30, or 90 nM of wild-type or mutant MCM protein (as monomer). After incubation at 60°C for 10 min, the mixture was filtered through an alkaline-washed nitrocellulose filter (Millipore, HA 0.45 μm) (McEntee et al. 1980) which was subsequently washed with 20 mM Tris–HCl (pH 7.5). The radioactivity adsorbed to the filter was measured by liquid scintillation counting. All DNA binding experiments were repeated three times, and their averages with standard deviations are shown in Figs. 2 and 5.

Helicase assay

Substrates for helicase assays were made as previously described (Shin et al. 2003b) by hybridizing two oligonucleotides, a 25mer 5′-CCGACGTGCCAGGCCGACGCGTCCC-3′ and a 50mer 5′-GGGACGCGTCGGCCTGGCACGTCGGCCGCTGCGGCCAGGCACCCGATGGC-3′. DNA helicase activity assays were measured in reaction mixtures (15 μl) containing 20 mM Tris–HCl (pH 8.5), 2 mM DTT, 10 mM $MgCl_2$, 100 μg/ml BSA, 3.33 mM ATP, 10 fmol (0.66 nM) of ^{32}P-labeled substrate and 10, 30 or 90 nM MCM protein (as monomer). After incubation at 60°C for 1 h, the reactions were stopped by adding 5 μl of loading buffer containing 1% SDS, 100 mM EDTA, 0.1% xylene cyanol, 0.1% bromophenol blue, and 50% glycerol, and chilled on ice. Aliquots (10 μl) were loaded onto an 8% native polyacrylamide gel in 0.5× TBE and electrophoresed for 40 min at 180 V. Gels were visualized and quantitated by phosphorimaging. All helicase experiments were repeated three times, and their averages with standard deviations are shown in Fig. 4a.

Differential scanning calorimetry (DSC) measurements

The purified proteins were dialyzed at room temperature against buffer containing 20 mM potassium phosphate (pH 7.5), 100 mM NaCl and 10% glycerol. Protein concentrations were determined using an absorbance at 280 nm and a calculated extinction coefficient of A_{280} of 28,730 cm^{-1} M^{-1}. The solution outside the dialysis bag was retained and used as reference for the experiments.

DSC measurements were performed using a VP-DSC Microcalorimeter from Microcal Inc. (Northampton, MA). The volume of the sample and the reference vessels was 0.511 ml and the scan was run either at slow (15 K h^{-1}) or at medium rate (60 K h^{-1}), with the temperature ranging from 25 to 85°C. Since the scans of protein samples were irreversible, the second scan for each sample was used as the baseline. After subtraction of the baseline from the protein scan, the resulting raw data of differential powers as a function of time were divided by the scan rate to convert into a heat capacity as a function of temperature.

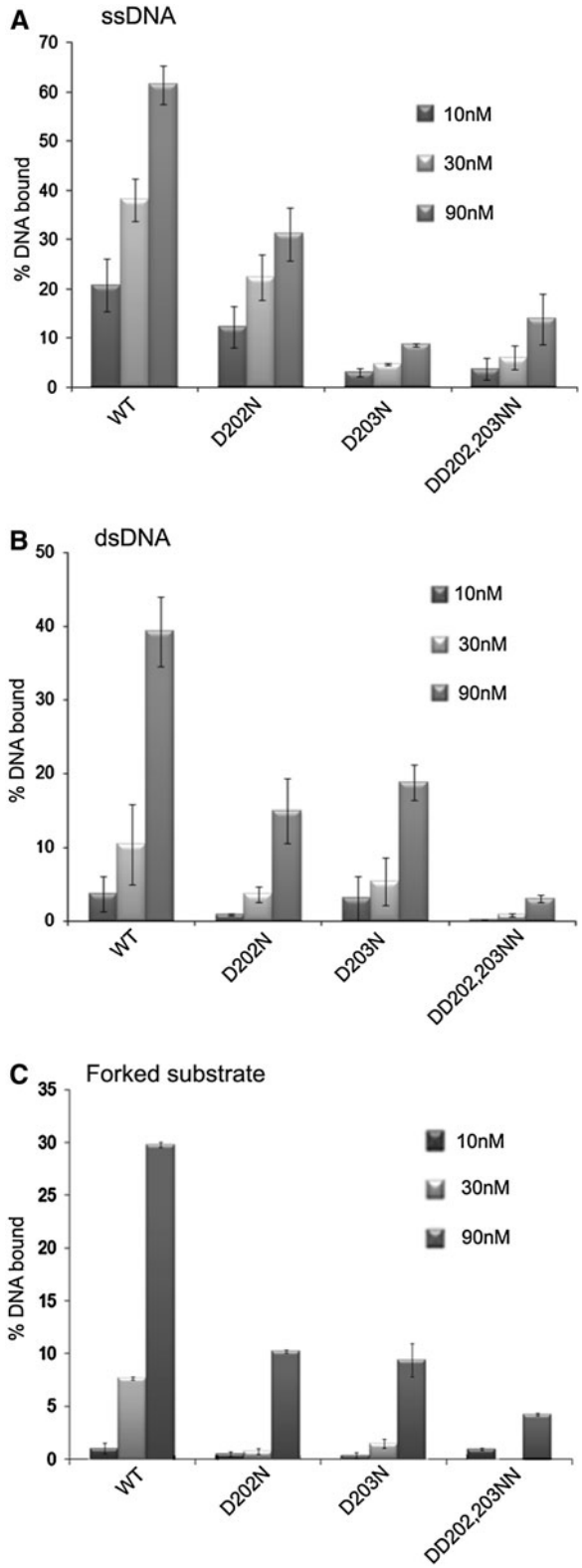

Fig. 2 Asp202 and Asp203 participate in DNA binding by mtMCM protein. Nitrocellulose filter binding assays were performed as described in "Materials and methods" using 50 fmol of ^{32}P-labeled single strand (**a**), double strand (**b**) or forked (**c**) DNA substrates in the presence of 10, 30, and 90 nM of protein (as monomer). The average of three independent experiments with standard deviations is shown

Utilizing the EXAM program (Kirchhoff 1993), a two-state, A ⇔ B, transition model was then fitted to the heat capacity as a function of temperature to determine the van't Hoff enthalpy (ΔH_{VH}) for the scan from the shape of the transition peak; a transition temperature (T_m) and a calorimetric transition enthalpy (ΔH_{cal}) were calculated from the area under the transition peak (mJ) divided by the moles of protein in the sample cell (concentration of protein × 0.511 ml). DSC scans on the samples were repeated twice.

Circular dichroism

Circular dichroism (CD) measurements were performed with a Model J-720 Jasco Spectropolarimeter using quartz cells with a 0.005 cm path length at room temperature. The proteins used for CD were prepared as described above for the DSC experiments, with concentrations of proteins ranging from 10 to 30 μM (as monomers). Far-UV wavelength scans were recorded at room temperature from 250 to 190 nm. Averages for three CD spectra were presented. Ellipticity results were expressed as mean residue ellipticity (θ) = degrees × centimeter^2 × decimole^{-1}.

Results

Mutations of residues Asp202 and Asp203 reduce DNA binding by mtMCM

During DNA unwinding, helicases bind and translocate along DNA. In mtMCM, it has been shown that two motifs found in the N-terminal region, zinc finger and β-hairpin motifs are important for DNA binding (Poplawski et al. 2001; Kasiviswanathan et al. 2006). It was suggested, however, that these are not the only regions of the mtMCM protein that interact with DNA. Using electron micrograph reconstruction, it was shown that DNA, particularly dsDNA, may also bind in the cleft between domains A and C (Costa et al. 2008). Since D202 and D203 are located in this cleft, they may participate in DNA binding. As shown in Fig. 2a, the D203N mutant protein and DD202,203NN double mutant protein show a significant decrease in ssDNA binding, although binding was not completely abolished. The D202N mutant protein binds ssDNA with about 50% of wild-type efficiency. When dsDNA was used as substrate, the double mutant (DD202,203NN) did not bind dsDNA (Fig. 2b), while the proteins with single mutations (D202N or D203N) bound dsDNA poorly compared to the wild-type enzyme (Fig. 2b). With both single-stranded and double-stranded substrates, the double mutant shows a more pronounced effect on DNA binding compared to the single mutants. It was reported that the

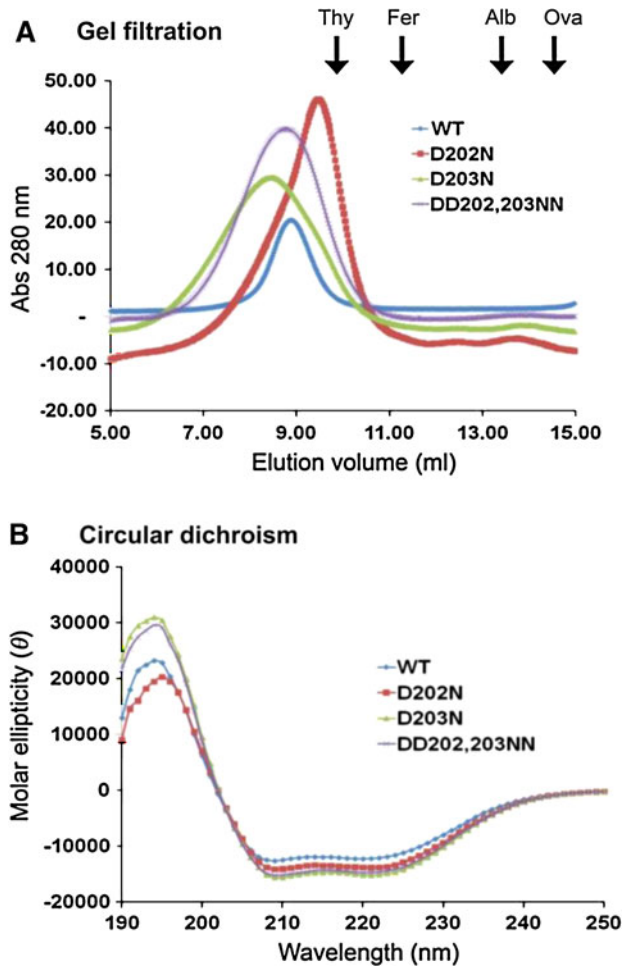

Fig. 3 Mutations of Asp 202 and 203 do not affect mtMCM protein structure. **a** The oligomeric states of the wild-type and mutant mtMCM proteins were determined using superose-6 gel filtration column as described in "Materials and methods". The elution positions of size markers are shown: thyroglobulin (Thy, 670,000 Da), ferritin (Fer, 440,000 Da), albumin (Alb, 67,000 Da) and ovalbumin (Ova, 45,000 Da). **b** The circular dichroism (CD) spectra of wild-type and mutant mtMCM proteins were measured as described in "Materials and methods"

Archaeoglobus fulgidus MCM binds fork-DNA substrate (origin-like substrate) better than ss or dsDNA substrate (Grainge et al. 2003; Rothenberg et al. 2007). However, the mutant MCM proteins bind forked substrates similar to ss and dsDNA, suggesting that the conserved Asp residues are not likely to be involved in substrate-specific interactions (Fig. 2c).

Mutating residues Asp202 and Asp203 do not affect the structural integrity of the mtMCM protein

Since residues D202 and D203 are located in the cleft between the domains A and B, they may be required for the overall structure of the protein. If the structure of the protein changes, it could explain the reduction in DNA binding by the mutant enzymes. To determine if the mutation causes a gross structural alteration, the secondary structure composition and the oligomeric structure of the wild-type and mutant proteins were analyzed. The elution profiles of the mutant proteins differ slightly (Fig. 3a). It has been shown that MCM protein is in dynamic equilibrium between different oligomeric states (Shin et al. 2009). It is likely that the small variation of the elution profile of the wild-type and mutant proteins from the sizing column is due to a subtle effect of the mutation on these dynamic equilibriums. The overall secondary structures of the proteins did not substantially change as all proteins exhibit similar CD profiles (Fig. 3b). Thus, the data suggest that the overall structures of the mtMCM molecules were not grossly affected by the mutations.

Table 1 The thermostability of wild-type and mutants mtMCM proteins

	T_m avg (°C)	ΔH_{VH} (kJ/mole)	ΔH_{cal} (kJ/mole)[a]
Wild type	66.2 ± 1.7[b]	1,246.8 ± 159.0	530.6 ± 3.1
D202N	63.7 ± 0.1	1,123.5 ± 149.2	276.6 ± 56.6
D203N	62.5 ± 0.2	1,360.0 ± 157.0	284.5 ± 3.2
DD202,203NN	57.2 ± 1.7[b]	1,277.5 ± 286.4	198.1 ± 48.3

[a] Calorimetric enthalpy is determined from measuring the absorbance of proteins at 280 nm and concentration was determined using the calculated extinction coefficient of mtMCM ($\varepsilon = 28{,}730$)

[b] The average of slow and medium scans

The mutant mtMCM proteins have reduced thermostability

Although mutating amino acids D202 and D203 do not affect the overall structure of the proteins, the sizing column and CD analysis were performed at ambient temperature. It is thus possible that the mutations may affect the thermostability of the enzymes at high temperature. DSC analysis shows that the wild-type protein has an average melting temperature (T_m) of 66.2°C (Table 1). The D202N, D203N and DD202,203NN mutant proteins showed reduced thermostability (average T_m of 63.7, 62.5, and 57.2°C, respectively) (Table 1), suggesting a role for D202 and D203 in mtMCM thermostability. Since the DNA binding assays were performed at 60°C, the DSC results may provide part of the explanation for the lower affinity for DNA by the mutant proteins; they are less stable at the experimental temperature.

Mutation of Asp202 and Asp203 does not affect mtMCM helicase activity

DNA binding by the helicase is required for helicase activity. Thus, one would expect that the reduced DNA

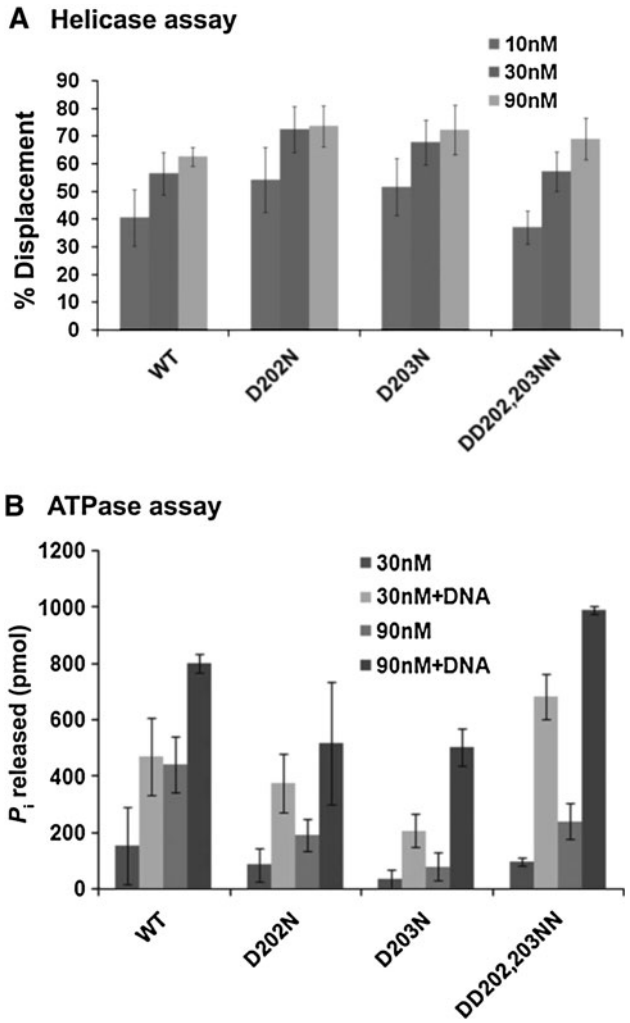

Fig. 4 Asp202 and Asp203 are not required for helicase or ATPase activity in the mtMCM protein. **a** Helicase activity was measured as described in "Materials and methods" using 10, 30, and 90 nM of wild-type or mutant mtMCM protein (as monomer). The average of three independent experiments with standard deviation is shown. **b** ATPase activity was measured as described in "Materials and methods" using 30 and 90 nM of wild-type or mutant mtMCM proteins (as monomer) in the presence or absence of 50 ng ssDNA. The average of three independent experiments with standard deviation is shown

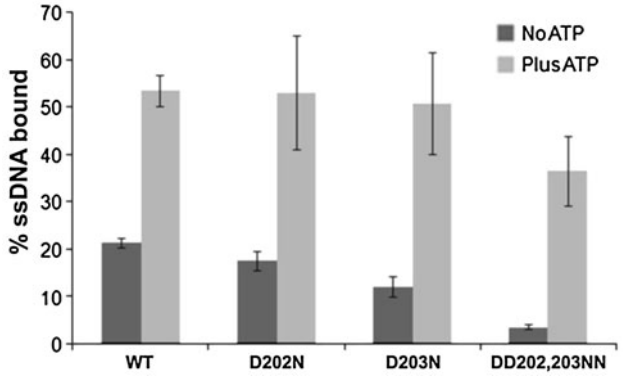

Fig. 5 DNA binding by mtMCM is modulated by ATP. Filter binding assays were performed as described under "Materials and methods" using 50 fmol of ^{32}P-labeled ssDNA in the presence of 25 nM wild-type or mutants mtMCM proteins (as monomer) in the absence or presence of 1 mM ATP. The average of three independent experiments with standard deviation is shown

binding observed with the mutant proteins (Fig. 2) would affect the mtMCM helicase activity. However, no significant effect on helicase activity was observed with the mutant proteins (Fig. 4a). On the other hand, there were some reductions in ATPase activities in the D202N and D203N mutants in the absence or presence of DNA (Fig. 4b). Despite these variations, the results suggest that the helicase and ATPase activities are not significantly affected by the mutations. Therefore, the activity results (Fig. 4) and the observation of reduced DNA binding caused by the mutations (Fig. 2) seem contradictory as DNA binding is required for helicase activity and the ATPase is known to be stimulated by DNA as also shown in Fig. 4b.

ATP stimulates DNA binding by the mutant mtMCM proteins

As mentioned above, although the mutant proteins were less stable at 60°C (Table 1) and reduced DNA binding was observed (Fig. 2), the mutant enzymes retained helicase activity (Fig. 4a). One of the differences between the DNA binding assays (Fig. 2) and the helicase and ATPase assays (Fig. 4) is the presence of ATP. It has been reported that ATP stimulates the binding of MCM to ssDNA when incubated at elevated temperature (Poplawski et al. 2001). It is thus possible that ATP affects the DNA binding by the mtMCM mutant proteins. As shown in Fig. 5, in the presence of ATP, the mutant proteins bind DNA as well as the wild-type enzyme, which may explain the efficient helicase activity observed with the mutant proteins. It is possible that ATP locally alters the structure of the mutant proteins, allowing them to bind to DNA and consequently translocate and unwind the duplex. In addition, it was shown that ATP enhances the thermostability of the helicase (Sakakibara et al. 2009b), which may also explain why the mutant enzymes can bind DNA at high temperature with a higher affinity in the presence of ATP.

Discussion

It is shown here that two conserved Asp residues in the N-terminal part of the MCM proteins play a role in DNA binding although they are not located in the central cavity of the helicase. Several lines of evidence, however, suggest

that DNA also interacts with the surface of the MCM ring. An electron microscopy study of mtMCM structure complexed with long dsDNA showed that DNA binds to the outer surface of MCM (Costa et al. 2008). Domain A (Fig. 1a) was shown to participate in DNA binding since deletion of domain A resulted in a significant decrease in DNA binding by mtMCM (Kasiviswanathan et al. 2004). It was also found that when the *Sulfolobus solfataricus* MCM protein was provided with a DNA substrate containing both 3′ and 5′ ssDNA overhanging regions, the 3′ ssDNA was located at the central cavity while the 5′ ssDNA was associated with the outer surface of the helicase (Rothenberg et al. 2007). The region of the MCM surface that interacts with the 5′-overhang region, however, is not yet clear. Our data also show that these mutant proteins have a negative impact on binding to forked substrate as well as ss and dsDNA (Fig. 2). This suggests that the Asp residues are not likely to be involved in specific interactions with specific substrates, but rather these residues seem to affect the global changes in MCM helicase interaction with DNA in the absence of ATP.

A previous study determined the role of another conserved residue, proline 62 (P62), for mtMCM function (Fletcher and Chen 2006). This residue is found in the interface between domain A and domain C in the mtMCM structure. P62 is the equivalent of proline 82 (P82) found in Mcm5 of *Saccharomyces cerevisiae*. Mutation of P82 to Leu (also known as the *Mcm5-Bob1* mutation) results in bypassing the requirement for the Dbf4-dependent Cdc7 kinase (DDK) activity that is essential for initiating DNA replication in yeast (Hardy et al. 1997; Fletcher et al. 2003). Biochemical analysis of the mtMCM P62L mutant enzyme showed reduced helicase activity but no effect on DNA binding (Fletcher and Chen 2006). When P62, D202 and D203 are mapped on the monomeric MCM, they are all located in the cleft between domains A and C (Fig. 6a). When the polar contacting residues of D202 and D203 were mapped, their side chains interact with neighboring residues in domain A (Fig. 6b). The side chain of D202 shows a hydrogen bond with an amine group from arginine at position 37. One of the oxygen molecules from the side chain of D203 forms hydrogen bonds with serine 38, while the other oxygen forms hydrogen bonds with R87. S38 forms a hydrogen bond with R87. Thus, in addition to P62 as an anchor point between domains A and C as suggested by Fletcher et al. 2003, it is possible that D202 and D203 also stabilize inter-domain interactions. The Asp202 residue is also conserved in human Mcm3 and Asp203 is conserved in human Mcm2, 3 and 4, while Mcm6 and 7 have a Glu residue at that position (Kasiviswanathan et al. 2004). It is thus likely that the role of these residues will also be conserved in the eukaryotic MCM proteins.

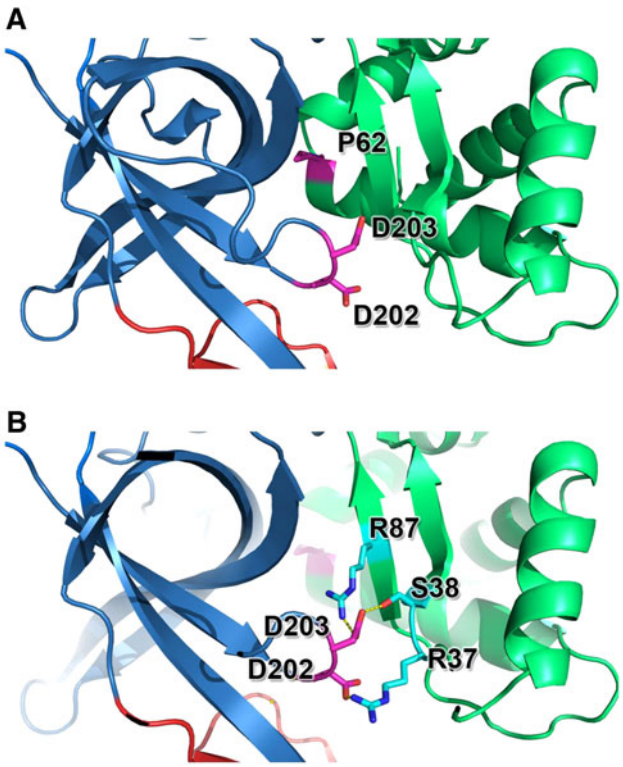

Fig. 6 Local interactions of the Asp202 and Asp203 residues on the three-dimensional structure of mtMCM protein. **a** Close up structure of the N-terminal part of the mtMCM protein is shown with domains represented in different colors. D202, D203 and P62 are labeled and shown with stick representation. See text for details. **b** Same view as part **a**, showing putative ionic interactions (*dotted line*) between side chains of D202 and R37; D203 and S38, and R87. R37, S38, and R87 are also labeled and shown in stick representation. See text for details

Moreover, it is shown here that the mutations of two conserved Asp residues in the cleft between domains A and C show ATP-dependent binding of DNA. One possible explanation for this dependence is the effect of ATP on the thermostability of the mutant proteins as was shown for the wild-type enzyme (Sakakibara et al. 2009b). The data presented here suggest that when the MCM protein binds to nucleotide in the catalytic domain, the conformation of domains A and C in the N-terminus is likely affected. It is possible that when the MCM protein is in the apo state (no nucleotide), domains A and C are floppy (less rigid) and have open states and thus cannot bind to DNA. The mutations at the cleft may augment this effect. However, when the nucleotide binds, the entire MCM protein structure becomes less flexible, including the interaction between domains A and C. This, in turn, may enable the enzyme to bind DNA.

Acknowledgments We would like to thank Dr. Lori Kelman for her comments on the manuscript. Specialty oligonucleotide synthesis was

supported as part of a NIST/UMD Joint Program in Bioscience Measurements (70NANB9H9196). This work was supported by a grant from the National Science Foundation (MCB-0815646).

References

Bae B et al (2009) Insights into the architecture of the replicative helicase from the structure of an archaeal MCM homolog. Structure 17:211–222

Brewster AS, Chen XS (2010) Insights into the MCM functional mechanism: lessons learned from the archaeal MCM complex. Crit Rev Biochem Mol Biol 45:243–256

Brewster AS et al (2008) Crystal structure of a near-full-length archaeal MCM: functional insights for an AAA+ hexameric helicase. Proc Natl Acad Sci USA 105:20191–20196

Costa A, Onesti S (2009) Structural biology of MCM helicases. Crit Rev Biochem Mol Biol 44:326–342

Costa A et al (2008) Cryo-electron microscopy reveals a novel DNA-binding site on the MCM helicase. EMBO J 27:2250–2258

Fletcher RJ, Chen XS (2006) Biochemical activities of the *BOB1* mutant in *Methanobacterium thermoautotrophicum* MCM. Biochemistry 45:462–467

Fletcher RJ, Bishop BE, Leon RP, Sclafani RA, Ogata CM, Chen XS (2003) The structure and function of MCM from archaeal *M. thermoautotrophicum*. Nat Struct Biol 10:160–167

Grainge I, Scaife S, Wigley DB (2003) Biochemical analysis of components of the pre-replication complex of *Archaeoglobus fulgidus*. Nucleic Acids Res 31:4888–4898

Hardy CF, Dryga O, Seematter S, Pahl PM, Sclafani RA (1997) *mcm5/cdc46-bob1* bypasses the requirement for the S phase activator Cdc7p. Proc Natl Acad Sci USA 94:3151–3155

Kasiviswanathan R, Shin JH, Melamud E, Kelman Z (2004) Biochemical characterization of the *Methanothermobacter thermautotrophicus* minichromosome maintenance (MCM) helicase N-terminal domains. J Biol Chem 279:28358–28366

Kasiviswanathan R, Shin JH, Kelman Z (2006) DNA binding by the *Methanothermobacter thermautotrophicus* Cdc6 protein is inhibited by the minichromosome maintenance helicase. J Bacteriol 188:4577–4580

Kelman LM, Kelman Z (2003) Archaea: an archetype for replication initiation studies? Mol Microbiol 48:605–615

Kirchhoff WH (1993) Exam: a two-state thermodynamic analysis program. NIST Tech Note 1401:1–103

Liu W, Pucci B, Rossi M, Pisani FM, Ladenstein R (2008) Structural analysis of the *Sulfolobus solfataricus* MCM protein N-terminal domain. Nucleic Acids Res 36:3235–3243

McEntee K, Weinstock GM, Lehman IR (1980) recA protein-catalyzed strand assimilation: stimulation by *Escherichia coli* single-stranded DNA-binding protein. Proc Natl Acad Sci USA 77:857–861

McGeoch AT, Bell SD (2008) Extra-chromosomal elements and the evolution of cellular DNA replication machineries. Nat Rev Mol Cell Biol 9:569–574

Poplawski A, Grabowski B, Long SE, Kelman Z (2001) The zinc finger domain of the archaeal minichromosome maintenance protein is required for helicase activity. J Biol Chem 276:49371–49377

Rothenberg E, Trakselis MA, Bell SD, Ha T (2007) MCM forked substrate specificity involves dynamic interaction with the 5′-tail. J Biol Chem 282:34229–34234

Sakakibara N, Kasiviswanathan R, Melamud E, Han M, Schwarz FP, Kelman Z (2008) Coupling of DNA binding and helicase activity is mediated by a conserved loop in the MCM protein. Nucleic Acids Res 36:1309–1320

Sakakibara N, Kelman LM, Kelman Z (2009a) Unwinding the structure and function of the archaeal MCM helicase. Mol Microbiol 72:286–296

Sakakibara N, Schwarz FP, Kelman Z (2009b) ATP hydrolysis and DNA binding confer thermostability on the MCM helicase (dagger). Biochemistry 48:2330–2339

Shin JH, Kelman Z (2006) The replicative helicases of bacteria, archaea and eukarya can unwind RNA–DNA hybrid substrates. J Biol Chem 281:26914–26921

Shin JH, Grabowski B, Kasiviswanathan R, Bell SD, Kelman Z (2003a) Regulation of minichromosome maintenance helicase activity by Cdc6. J Biol Chem 278:38059–38067

Shin JH, Jiang Y, Grabowski B, Hurwitz J, Kelman Z (2003b) Substrate requirements for duplex DNA translocation by the eukaryal and archaeal minichromosome maintenance helicases. J Biol Chem 278:49053–49062

Shin JH, Heo GY, Kelman Z (2009) The *Methanothermobacter thermautotrophicus* MCM helicase is active as a hexameric ring. J Biol Chem 284:540–546